Fingerprints of Qubit Noise in Transient Cavity Transmission

Philipp M. Mutter [*] and Guido Burkard [†]
Department of Physics, University of Konstanz, D-78457 Konstanz, Germany

(Received 21 January 2022; accepted 10 May 2022; published 8 June 2022)

Noise affects the coherence of qubits and thereby places a bound on the performance of quantum computers. We theoretically study a generic two-level system with fluctuating control parameters in a photonic cavity and find that basic features of the noise spectral density are imprinted in the transient transmission through the cavity. We obtain analytical expressions for generic noise and proceed to study the cases of quasistatic, white and $1/f^{\alpha}$ noise in more detail. Additionally, we propose a way of extracting the noise power spectral density in a frequency band only bounded by the range of the qubit-cavity detuning and with an exponentially decaying error due to finite measurement times. Our results suggest that measurements of the time-dependent transmission probability represent a novel way of extracting noise characteristics.

DOI: 10.1103/PhysRevLett.128.236801

A main threat to large-scale quantum computation is noise-induced decoherence of the qubit state [1,2]. Common noise sources include fluctuating electromagnetic fields that arise from noisy control parameters as well as the interaction with the environment, e.g., $1/f$ noise due to two-state fluctuators in the material [3], the nuclear spin bath in semiconductor quantum dots [4–6], and magnetic flux noise, quasiparticles, and two-level fluctuators in superconducting circuits [7–10]. Noise may even affect spin qubits in isotopically purified materials as the spin-orbit interaction couples the spin and charge, thus introducing charge noise to the system [11,12]. Relevant examples are hole spins in germanium [13–20].

With quantum error correction still a long way off, the characterization and suppression of noise is of the utmost importance in intermediate-scale quantum devices [21–23]. In this Letter, we propose a novel way of extracting noise characteristics using the cavity transmission which has been used for the dispersive readout of quantum systems [24–27] as well as for the determination of system parameters [28,29] and to detect signatures of the strong coupling regime of cavity quantum electrodynamics [27,30–33]. We go beyond the standard steady-state case and demonstrate that fluctuations affecting the qubit leave a clear trace in the transient transmission. Our model is generally applicable to a wide range of cavity-coupled qubit systems, and in contrast to established noise spectroscopy techniques such as the filter function formalism or relaxometry [34], our method does not require many high-fidelity pulses for dynamical decoupling [35–39], nor do we have to make any assumptions on the noise, e.g., it is not necessary to restrict the analysis to weak or Markovian noise.

We study a single mode of an electromagnetic cavity with frequency ω_c interacting with an infinite number of external modes. A qubit affected by noise is placed inside the cavity and interacts with the cavity mode (Fig. 1). We consider both transverse and longitudinal qubit-photon couplings. In the absence of external driving, in a frame corotating with the probe field at frequency ω_p, and within the rotating wave approximation, only the transverse coupling g is relevant, and the cavity-coupled two-level system is described by the Hamiltonian

$$H = [\omega_q + \delta\omega_q(t) - \omega_p]\sigma_z/2 + \Delta a^\dagger a + g(a\sigma_+ + a^\dagger\sigma_-), \tag{1}$$

where $\Delta = \omega_c - \omega_p$ is the cavity-probe detuning, σ_z the Pauli Z matrix, a the photon annihilation operator, and σ_- a ladder operator acting on the qubit. The qubit energy separation is affected by noise, $\omega_q + \delta\omega_q(t)$, and the fluctuating component may be written to leading order as $\delta\omega_q(t) = \lambda\delta X(t)$, where $\delta X(t)$ is the dynamical noise that couples to the qubit control parameter X with strength $\lambda = \partial_X \omega_q|_{\delta X=0}$. The qubit-cavity coupling can also be affected by noise, and we will take this into account further below. As is shown in the Supplemental Material [40], the system is well described by the quantum Langevin equations for the expectation values of the operators σ_- and a,

$$\begin{aligned}\frac{d\langle\sigma_-\rangle}{dt} &= -i[\omega_q + \delta\omega_q(t) - \omega_p]\langle\sigma_-\rangle - \frac{\gamma}{2}\langle\sigma_-\rangle + ig\langle\sigma_z\rangle\langle a\rangle,\\ \frac{d\langle a\rangle}{dt} &= -i\Delta\langle a\rangle - \frac{\kappa}{2}\langle a\rangle - ig\langle\sigma_-\rangle + \sqrt{\kappa_1}\langle b_{\mathrm{in}}(t)\rangle,\end{aligned} \tag{2}$$

where γ is the total noise-independent qubit decoherence rate [41], and $\kappa = \kappa_1 + \kappa_2$ is the total cavity loss rate given by the sum of the rates κ_j at port $j \in \{1, 2\}$. $\langle\sigma_z\rangle$ can depend on time but knowledge of its specific form is not

 © 2022 American Physical Society

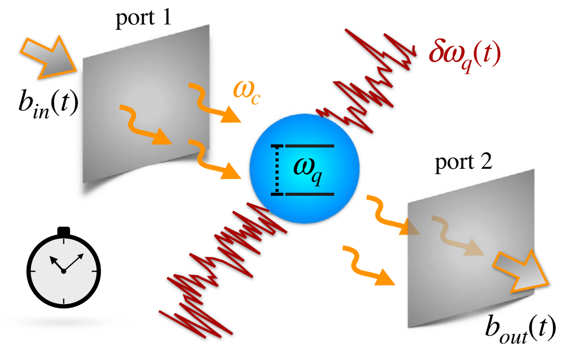

FIG. 1. A two-level system (qubit, shown in blue) with energy splitting ω_q is affected by noise $\delta\omega_q$ (red) and is placed inside a single-mode electromagnetic cavity with frequency ω_c. Partially transparent mirrors allow for the interaction of the qubit-cavity system with external modes. An input field $b_{\mathrm{in}}(t)$ enters at port 1, causing an output field $b_{\mathrm{out}}(t)$ that leaves the cavity at port 2, thereby creating a time-dependent transmission through the system from left to right.

required for computing the transmission within the perturbative approach presented below. The bath input field at port 1 is chosen to be a plane wave and hence a constant in the rotating frame, $\langle b_{\mathrm{in}}(t)\rangle = \langle b_{\mathrm{in}}\rangle$, while we assume no input field to be present at port 2.

By solving the system of coupled differential equations (2), one may obtain the cavity transmission amplitude by employing input-output theory [42–44], $A(t) = \langle b_{\mathrm{out}}(t)\rangle/\langle b_{\mathrm{in}}(t)\rangle = -\sqrt{\kappa_2}\langle a(t)\rangle/\langle b_{\mathrm{in}}(t)\rangle$. An exact solution of Eq. (2) cannot be obtained for generic noise. Working in the regime where the qubit-cavity coupling is small compared to the dominant energy scale, $|g| \ll \eta \equiv \max\{|\delta_0|, |\kappa-\gamma|\}$ with the unperturbed qubit-cavity detuning $\delta_0 = \omega_c - \omega_q$, we may solve Eq. (2) perturbatively to leading order in g/η,

$$\begin{aligned} A(t) &= \frac{\sqrt{\kappa_1\kappa_2}}{i\Delta + \kappa/2}(e^{-i\Delta t - \kappa t/2} - 1) \\ &\quad - \frac{\sqrt{\kappa_2}}{\langle b_{\mathrm{in}}\rangle} e^{-i\Delta t - \kappa t/2}[\langle a(0)\rangle - ig\langle\sigma_-(0)\rangle\mathcal{I}(t)], \\ \mathcal{I}(t) &= \int_0^t e^{i\delta_0 t' + (\kappa-\gamma)t'/2 - i\lambda\mathcal{X}(t')} dt'. \end{aligned} \tag{3}$$

Here, $\langle\sigma_-(0)\rangle$ and $\langle a(0)\rangle$ are initial conditions, and we introduce the noise integral $\mathcal{I}(t)$ containing the stochastic phase $\mathcal{X}(t) = \int_0^t \delta X(t')dt'$. There are a few remarks in order here: (i) Although we treat g perturbatively, this does not mean that our approach does not contain strong coupling cases with $|g| > \kappa$, γ. There, the approximation remains sound if $|g| \ll |\delta_0|$. (ii) To leading order in g the long-time solution is unchanged by the noise, and only the transient transmission allows for a determination of noise characteristics. The transient phase generally lasts for a time $\sim 1/\kappa$, but the decay of the noise integral also depends on γ and the details of the noise as discussed below. The minimum detection time interval T_d decreases with increasing κ_2 and signal-to-noise ratio (SNR), $T_d \sim 1/(\kappa_2 \mathrm{SNR})$ [45,46], and it must be smaller than the typical timescale on which the noise changes, a condition that can be particularly restrictive for high-frequency noise. The number of data points N attainable in the transient phase is then determined by the SNR of the detector, $N \sim (1/\kappa)/T_d \sim \mathrm{SNR}$, and SNRs exceeding 10^2 have been reported in the solid-state literature [45,47,48]. Additionally, the finite time averaging process dictates a maximum detuning δ_0^m, and for $\kappa \sim \gamma$ we require $g \ll \delta_0^m \sim 1/T_d$ for our results to be valid. (iii) Even at this point we can see the role of the initial qubit state. For $\langle\sigma_-(0)\rangle$ to be nonvanishing, we need the qubit to be initialized in a coherent superposition of its energy eigenstates, and in the following we assume $\langle\sigma_-(0)\rangle = 1/2$. Moreover, we assume that $\langle a(0)\rangle = 0$, e.g., the cavity may initially be empty. (iv) There are two quantities in Eq. (2) that are affected by finite temperature effects: the qubit level population $\langle\sigma_z(t)\rangle$ and the decoherence rate γ. The former appears in the expansion of $\langle a(t)\rangle$ only at higher orders in perturbation theory, and the latter is only altered in magnitude at increased thermal energies, while the form of the Langevin equations is unchanged. As a result, Eq. (3) also describes the noisy transmission at finite temperature. Remarkably, temperature does not wash out the noise traces in the transient cavity transmission in magnitude. However, an increased γ can lead to a quickly decaying noise signal, hence requiring small measurement times.

Averaging over the noise is possible once we consider an observable quantity, such as the transmission probability $|A|^2$ that will be investigated here. We remark that since the zeroth-order term in Eq. (3) is not affected by noise one has $\langle\langle|A|^2\rangle\rangle = \langle\langle|A|\rangle\rangle^2$ to first order in g/η, and hence the variance of $|A|$ vanishes. In general, the kth central moment of $|A|$ can become nonzero only at order k or higher in g/η, implying $\langle\langle|A|^k\rangle\rangle = \langle\langle|A|\rangle\rangle^k + \mathcal{O}[(g/\eta)^2]$ [40]. In present-day two-level systems one may expect $\gamma \sim \kappa \sim g \sim \mathrm{MHz}$ [27]. For the perturbative approach to be valid we then must consider the dispersive regime, $|\delta_0| \gg |g|$. Assuming symmetric mirrors $\kappa_1 = \kappa_2 = \kappa/2$ and choosing $\langle b_{\mathrm{in}}\rangle$ to be real, we obtain up to leading order in g/η,

$$\langle\langle|A(t)|\rangle\rangle = |A_\infty|\sqrt{\xi_0(t) + \xi_1(t)}. \tag{4}$$

Here, $|A_\infty| = \kappa/\sqrt{4\Delta^2 + \kappa^2}$ is the Lorentz-shaped transmission through an empty cavity at long times $\kappa t \gg 1$, and we introduce the quantities

$$\begin{aligned} \xi_0(t) &= 1 + e^{-\kappa t} - 2e^{-\kappa t/2}\cos\Delta t, \\ \xi_1(t) &= \frac{g e^{-\kappa t/2}}{\sqrt{2/\kappa}\langle b_{\mathrm{in}}\rangle}[F(t)\mathrm{Re}\langle\langle\mathcal{I}(t)\rangle\rangle + G(t)\mathrm{Im}\langle\langle\mathcal{I}(t)\rangle\rangle], \\ F(t) &= \frac{2\Delta}{\kappa}(\cos\Delta t - e^{-\kappa t/2}) - \sin\Delta t, \\ G(t) &= \cos\Delta t - e^{-\kappa t/2} + \frac{2\Delta}{\kappa}\sin\Delta t. \end{aligned} \tag{5}$$

$\xi_0(t)$ describes the transient signal of an empty cavity, while $\xi_1(t)$ is a correction term due to the interaction with the noisy qubit. The latter can be seen as the normalized fluctuations in the averaged transmission probability,

$$\xi_1 = \frac{\langle\langle |A|^2 \rangle\rangle - |A_\infty|^2 \xi_0}{|A_\infty|^2} = \frac{\delta\langle\langle |A|^2 \rangle\rangle}{|A_\infty|^2}, \tag{6}$$

and features the averaged noise integral (ANI),

$$\langle\langle \mathcal{I}(t) \rangle\rangle = \int_0^t e^{i\delta_0 t' + (\kappa-\gamma)t'/2} \langle\langle e^{-i\lambda \mathcal{X}(t')} \rangle\rangle dt', \tag{7}$$

where $\langle\langle \ldots \rangle\rangle$ denotes the average over many measurements. Since only first-order processes are taken into account and single photons hence cannot contain noise correlations, only the averaged fluctuations ξ_1 allow for a characterization of noise features. In order to be able to neglect the g^2 term when expanding the absolute value squared of the transmission amplitude (3) while still suppressing higher orders in the perturbation expansion, we require $\sqrt{\kappa}/\langle b_{\rm in} \rangle \sim 1$. This restriction, however, is not severe as $\langle b_{\rm in} \rangle$ may be tuned externally and independently of the remaining parameters. Equation (4) describes the transmission for quite general systems and without any specifications of the noise $\delta X(t)$ or the corresponding stochastic phase $\mathcal{X}(t)$, and it is shown for exemplary parameter settings in Fig. 2. By recording the noisy part of the transmission via comparison with the transmission through an empty cavity for two distinct detunings Δ_1 and Δ_2, one may extract the real and imaginary part of the ANI for any δ_0 up to a desired maximum time t_m by choosing $|\Delta_2 - \Delta_1| t_m < \pi$ [40].

Up to this point the linearized noise has been treated exactly. In many realistic systems, however, noise affecting ω_q will also affect g. Writing $g \to g + \delta g(t)$, where to leading order $\delta g(t) = \lambda' \delta X(t)$ with $\lambda' = \partial_X g|_{\delta X = 0}$, we may work to first order in δg and integrate by parts to obtain an additional term in the averaged transmission [40],

$$\langle\langle |A(t)| \rangle\rangle = |A_\infty| \sqrt{\xi_0(t) + \xi_1(t) + \xi_1'(t)}, \tag{8}$$

where $\xi_0(t)$ and $\xi_1(t)$ are as given in Eq. (5) and

$$\xi_1'(t) = \frac{\lambda'}{\lambda} \frac{e^{-\kappa t/2}}{\sqrt{2/\kappa} \langle b_{\rm in} \rangle} \mathcal{F}(t) \tag{9}$$

with

$$\begin{aligned} \mathcal{F}(t) = {} & e^{(\kappa-\gamma)t/2} \langle\langle e^{-i\lambda \mathcal{X}(t)} \rangle\rangle [G(t)\cos\delta_0 t - F(t)\sin\delta_0 t] \\ & + G(t)\left[\delta_0 \mathrm{Im}\langle\langle \mathcal{I}(t) \rangle\rangle - \frac{\kappa-\gamma}{2}\mathrm{Re}\langle\langle \mathcal{I}(t) \rangle\rangle - 1\right] \\ & + F(t)\left[\delta_0 \mathrm{Re}\langle\langle \mathcal{I}(t) \rangle\rangle + \frac{\kappa-\gamma}{2}\mathrm{Im}\langle\langle \mathcal{I}(t) \rangle\rangle\right]. \end{aligned} \tag{10}$$

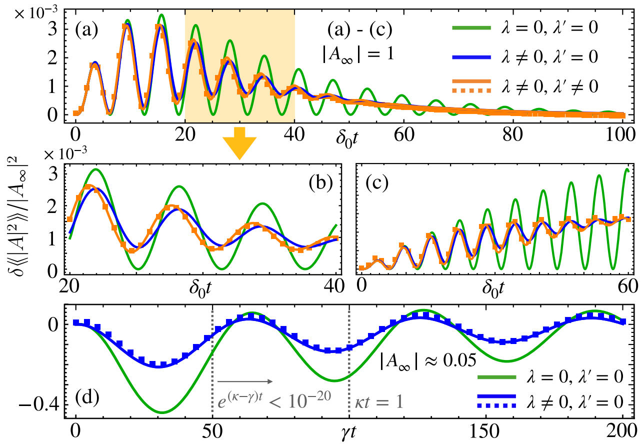

FIG. 2. The normalized fluctuations in the averaged transmission probability $\delta\langle\langle |A|^2 \rangle\rangle / |A_\infty|^2 = \xi_1 + \xi_1'$ as a function of time. We compare the cases of a noise-free (green) and noisy (blue/orange) qubit placed inside the cavity. Solid lines are drawn according to Eqs. (5) (blue) and (9) (orange). Squares are numerical results obtained by averaging over 10^3 exact solutions of the full Lindblad equation, allowing for up to 12 cavity photons and assuming normally distributed quasistatic noise with zero mean and standard deviation $\delta X_{\rm rms} = 0.05\delta_0$. (a) The complete first-order transient curve for the case $g = 0.1\kappa = 0.1\gamma = 0.01\delta_0$ at $\Delta = 0$. We find excellent agreement between the analytical and numerical results, even in the presence of a fluctuating coupling constant as can be seen from the magnified section of the plot in panel (b). (c) The initial first-order transient curve for the strong coupling case $g = \kappa = \gamma = 0.01\delta_0$ at $\Delta = 0$. (d) The first-order transient curve for $g = \kappa = 0.01\gamma$ at $\delta_0 = \Delta = 0.1\gamma$ with $\delta X_{\rm rms} = \gamma$. The remaining parameter values used are $\langle \sigma_z(0) \rangle = 0$, $\lambda = 0.9$, $\lambda' = -0.1$, $\omega_q/T = 1$, and $\sqrt{\kappa}/\langle b_{\rm in} \rangle = 1$.

In this case the fluctuations are $\delta\langle\langle |A|^2 \rangle\rangle / |A_\infty|^2 = \xi_1 + \xi_1'$ in analogy to Eq. (6). While we must treat the noise in g perturbatively, this is not a severe restriction since the fluctuations in g are expected to be bounded by the coupling itself, $\delta g = \lambda' \delta X < g$. The effect of noise in the energy separation and the qubit photon coupling on the averaged transmission can be clearly seen in Fig. 2(b). At the double resonance $\Delta = \delta_0 = 0$ the term ξ_1 vanishes identically, and for weak coupling ξ_1' is the dominant contribution.

Having obtained an expression for the measurable average transmission probability for generic longitudinal qubit noise affecting the energy separation and the coupling constant, we proceed to study the averaged phase (AP) $\langle\langle e^{-i\lambda \mathcal{X}(t)} \rangle\rangle$ and the ANI $\langle\langle \mathcal{I}(t) \rangle\rangle$ in more detail. The stochastic phase $\mathcal{X}(t)$ is defined as the time integral over the noise $\delta X(t)$ which is assumed to have zero mean in the remainder of this Letter. When the autocorrelations $\langle\langle \delta X(0) \delta X(\tau) \rangle\rangle$ decay on timescales τ_c which are small compared to the time of integration, the random phase is a sum of many independent random variables. In this situation the central limit theorem guarantees that the probability distribution of $\mathcal{X}(t)$ is Gaussian, and we may write for the AP [49,50]

$$\langle\langle e^{-i\lambda\mathcal{X}(t)}\rangle\rangle = \exp\left[-\frac{\lambda^2}{2\pi}\int_0^\infty \frac{\sin^2(\omega t/2)}{(\omega/2)^2}S(\omega)d\omega\right], \quad (11)$$

where $S(\omega)$ is the noise spectral density, given by the Fourier transform of the noise autocorrelator. Since the lower integration bound is zero, the Gaussian approximation is not expected to hold at measurement times t that are of the same order as the noise correlation time τ_c. Instead, the condition $\tau_c \ll t$ must be met for Eq. (11) to accurately describe the stochastic phase in the transient cavity transmission. On the other hand, $\delta X(t)$ itself may be the sum of many uncorrelated microscopic modes. In this case $\mathcal{X}(t)$ will follow Gaussian statistics regardless of the integration time t. If none of the above conditions are met, one must go beyond the Gaussian approximation [51].

There are two prominent special cases for which the ANI in the Gaussian approximation may be explored further analytically, quasistatic noise and white noise. We first consider the case of quasistatic noise [52]. Assuming the total integration time t to be smaller than the time scale on which the quasistatic noise changes, the ANI becomes a Gaussian and may be evaluated,

$$\langle\langle\mathcal{I}(t)\rangle\rangle_{\mathrm{qs}} = \sqrt{\frac{\pi}{2}}\frac{e^{Y^2}}{\lambda\delta X_{\mathrm{rms}}}\left[\mathrm{erf}(Y) + \mathrm{erf}\left(\frac{\lambda\delta X_{\mathrm{rms}}t}{\sqrt{2}} - Y\right)\right], \quad (12)$$

where $Y = [i\delta_0 + (\kappa-\gamma)/2]/\sqrt{2}\lambda\delta X_{\mathrm{rms}}$, $\delta X_{\mathrm{rms}} = \sqrt{\langle\langle\delta X^2\rangle\rangle}$ is the root mean square of the noise, and erf denotes the error function. We now turn to the case of white noise, where $S = S_0$ is constant. The exponent of the AP becomes linear in time, yielding the exact expression for the ANI,

$$\langle\langle\mathcal{I}(t)\rangle\rangle_w = \frac{e^{i\delta_0 t + (\kappa-\gamma)t/2 - \lambda^2 S_0 t/2} - 1}{i\delta_0 + (\kappa-\gamma)/2 - \lambda^2 S_0/2}. \quad (13)$$

For $S_0 = 0$, Eq. (13) is the ANI in the noise-free case. As white noise describes a Markovian process, it only renormalizes the qubit decoherence rate γ stemming from the Lindblad formalism, $\gamma \to \gamma + \lambda^2 S_0$.

Next, we investigate generic noise. In real measurements, data cannot be acquired over an infinitely broad frequency band. This can be taken into account by introducing an ultraviolet (uv) cutoff in Eq. (11), i.e., by shifting the upper integration bound from infinity to ω_{uv}. For $\omega_{\mathrm{uv}} t \ll 1$, the sine function in Eq. (11) may be expanded around zero. Taking into account the leading term in the expansion, the exponent of the AP becomes quadratic in time and the ANI may be evaluated,

$$\langle\langle\mathcal{I}(t)\rangle\rangle = \frac{\pi}{\sqrt{2P}}\frac{e^{Z^2}}{\lambda}\left[\mathrm{erf}(Z) + \mathrm{erf}\left(\sqrt{\frac{P}{2\pi}}\lambda t - Z\right)\right], \quad (14)$$

where $Z = \sqrt{\pi/2P}[i\delta_0 + (\kappa-\gamma)/2]/\lambda$ and $P = \int S(\omega)d\omega$ is the noise power in the band $[0, \omega_{\mathrm{uv}}]$. As noise in quantum computation must be considered over a large bandwidth corresponding to gate operation times, the noise power P provides a practical figure of merit for the comparison of quantum information platforms [53]. Realistically, the condition $\omega_{\mathrm{uv}} t \ll 1$ can be fulfilled for spectra dominated by low frequencies such as $1/f^\alpha$ noise [54], which is ubiquitous in solid-state systems [3,55,56]. In these cases an additional infrared cutoff ω_{ir} is needed to regularize the power integral [57,58], justified, e.g., by finite data acquisition times [59]. For instance, for $S = C/\omega$ one has $P = C\ln(\omega_{\mathrm{uv}}/\omega_{\mathrm{ir}})$.

Finally, we consider arbitrary detunings δ_0. Truncation of the perturbation expansion is valid in the regime $g \ll |\kappa-\gamma|$, which is often realized through $\gamma \gg \kappa \sim g$ in solid-state qubits. Suppose that the ANI has been characterized for at least three values of the noise coupling strength λ which is controllable by external parameters. One may then consider the second derivative of the ANI,

$$\left.\frac{d^2\langle\langle\mathcal{I}(t,\delta_0)\rangle\rangle}{d\lambda^2}\right|_{\lambda=0} = e^{i\delta_0 t + (\kappa-\gamma)t/2}\zeta(t) + \frac{16}{\pi(\kappa-\gamma+2i\delta_0)} \times \int_0^\infty \frac{S(\omega)}{(\kappa-\gamma+2i\delta_0)^2 + 4\omega^2}d\omega, \quad (15)$$

where $\zeta(t)$ is a function that is upper bounded by a quadratic scaling in t. Hence, the relative error caused by neglecting the first term is upper bounded by the scaling $|\kappa-\gamma|^2 t^2 e^{(\kappa-\gamma)t/2}$, and for measurement times t with $\kappa t \sim 1 \ll (\gamma-\kappa)t$ it can be safely neglected, while the effect of the noise on the transmission is still visible [Fig. 2(d)]. By employing a partial fraction decomposition and using the symmetry of $S(\omega) = S(-\omega)$, the nonvanishing part of Eq. (15) may be rewritten as [40]

$$\left.\frac{d^2\langle\langle\mathcal{I}(\delta_0)\rangle\rangle}{d\lambda^2}\right|_{\lambda=0} = \frac{16}{(\kappa-\gamma+2i\delta_0)^2}\mathcal{C}(\delta_0), \quad (16)$$

where $\mathcal{C}(\delta_0) = (S\star K)(\delta_0)$ denotes the convolution of S with the kernel $K(\delta_0) = (\kappa-\gamma+2i\delta_0)^{-1}$. After Fourier transforming the kernel analytically, we may apply the convolution theorem to obtain

$$S(\omega) = -4\int_0^\infty \tilde{\mathcal{C}}(\tau)\cos(\omega\tau)e^{(\gamma-\kappa)\tau/2}d\tau, \quad (17)$$

where $\tilde{\mathcal{C}}(\tau)$ denotes the Fourier transform of the measurable convolution. Hence, S can be obtained by extracting $\mathcal{C}(\delta_0)$ and its Fourier transform from $\langle\langle|A|\rangle\rangle$ and evaluating (17). A numerically reconstructed spectral density is shown in

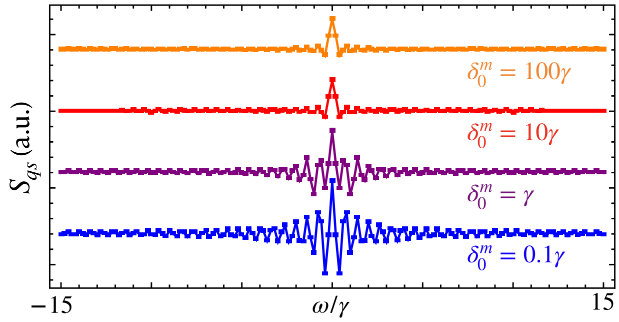

FIG. 3. A numerical reconstruction of S for quasistatic noise using the parameters in Fig. 2(d) at $\kappa t = 1$. The accuracy is determined by the maximum detuning δ_0^m available in experiment as indicated in the figure. The theoretical result is $S_{qs}(\omega) = 2\pi\delta X_{\mathrm{rms}}^2\delta(\omega)$, and the method based on Eq. (17) reproduces this form via the nascent delta function $(\tau_m/\pi)\mathrm{sinc}(\omega\tau_m)$ as the upper integration bound τ_m approaches infinity. The curves are shifted by constant values for clarity.

Fig. 3. Finite detection times do not introduce any additional restrictions on δ_0 and γ, and the results remain valid if $T_d \ll \min\{1/\kappa, 1/\Delta\}$ [40].

Future research may assess the effect of quantum noise on the transmission. In this case S can have an antisymmetric contribution and its extraction is not possible using the scheme described in this Letter. Additionally, given the overarching goal of noise mitigation one may investigate whether the qubit coherence in the presence of noise can be protected by the cavity photons.

We thank M. Benito for helpful discussions on the numerical solution of the Lindblad equation and J. R. Petta for insightful comments regarding finite detection times. This research is supported by the German Research Foundation [Deutsche Forschungsgemeinschaft (DFG)] under Project No. 450396347 and No. 425217212-SFB 1432.

*philipp.mutter@uni-konstanz.de
†guido.burkard@uni-konstanz.de

[1] W. H. Zurek, Decoherence, einselection, and the quantum origins of the classical, Rev. Mod. Phys. **75**, 715 (2003).
[2] P. Huang, Dephasing of exchange-coupled spins in quantum dots for quantum computing, Adv. Quantum Technol. **4**, 2100018 (2021).
[3] E. Paladino, Y. M. Galperin, G. Falci, and B. L. Altshuler, $1/f$ noise: Implications for solid-state quantum information, Rev. Mod. Phys. **86**, 361 (2014).
[4] C. Kloeffel and D. Loss, Prospects for spin-based quantum computing in quantum dots, Annu. Rev. Condens. Matter Phys. **4**, 51 (2013).
[5] X. Zhang, H.-O. Li, G. Cao, M. Xiao, G.-C. Guo, and G.-P. Guo, Semiconductor quantum computation, Natl. Sci. Rev. **6**, 32 (2019).
[6] G. Burkard, T. D. Ladd, J. M. Nichol, A. Pan, and J. R. Petta, Semiconductor spin qubits, arXiv:2112.08863.
[7] J. Clarke and F. K. Wilhelm, Superconducting quantum bits, Nature (London) **453**, 1031 (2008).
[8] W. D. Oliver and P. B. Welander, Materials in superconducting quantum bits, MRS Bull. **38**, 816 (2013).
[9] P. Krantz, M. Kjaergaard, F. Yan, T. P. Orlando, S. Gustavsson, and W. D. Oliver, A quantum engineer's guide to superconducting qubits, Appl. Phys. Rev. **6**, 021318 (2019).
[10] S. E. de Graaf, L. Faoro, L. B. Ioffe, S. Mahashabde, J. J. Burnett, T. Lindström, S. E. Kubatkin, A. V. Danilov, and A. Y. Tzalenchuk, Two-level systems in superconducting quantum devices due to trapped quasiparticles, Sci. Adv. **6**, eabc5055 (2020).
[11] P. Huang and X. Hu, Electron spin relaxation due to charge noise, Phys. Rev. B **89**, 195302 (2014).
[12] M. Benito, X. Croot, C. Adelsberger, S. Putz, X. Mi, J. R. Petta, and G. Burkard, Electric-field control and noise protection of the flopping-mode spin qubit, Phys. Rev. B **100**, 125430 (2019).
[13] N. Hendrickx, D. Franke, A. Sammak, G. Scappucci, and M. Veldhorst, Fast two-qubit logic with holes in germanium, Nature (London) **577**, 487 (2020).
[14] N. Hendrickx, W. Lawrie, L. Petit, A. Sammak, G. Scappucci, and M. Veldhorst, A single-hole spin qubit, Nat. Commun. **11**, 3478 (2020).
[15] P. M. Mutter and G. Burkard, Cavity control over heavy-hole spin qubits in inversion-symmetric crystals, Phys. Rev. B **102**, 205412 (2020).
[16] N. W. Hendrickx, W. I. Lawrie, M. Russ, F. van Riggelen, S. L. de Snoo, R. N. Schouten, A. Sammak, G. Scappucci, and M. Veldhorst, A four-qubit germanium quantum processor, Nature (London) **591**, 580 (2021).
[17] P. M. Mutter and G. Burkard, Natural heavy-hole flopping mode qubit in germanium, Phys. Rev. Research **3**, 013194 (2021).
[18] D. Jirovec, A. Hofmann, A. Ballabio, P. M. Mutter, G. Tavani, M. Botifoll, A. Crippa, J. Kukucka, O. Sagi, F. Martins, J. Saez-Mollejo, I. Prieto, M. Borovkov, J. Arbiol, D. Chrastina, G. Isella, and G. Katsaros, A singlet-triplet hole spin qubit in planar Ge, Nat. Mater. **20**, 1106 (2021).
[19] P. M. Mutter and G. Burkard, All-electrical control of hole singlet-triplet spin qubits at low-leakage points, Phys. Rev. B **104**, 195421 (2021).
[20] D. Jirovec, P. M. Mutter, A. Hofmann, A. Crippa, M. Rychetsky, D. L. Craig, J. Kukucka, F. Martins, A. Ballabio, N. Ares, D. Chrastina, G. Isella, G. Burkard, and G. Katsaros, Dynamics of Hole Singlet-Triplet Qubits with Large g-Factor Differences, Phys. Rev. Lett. **128**, 126803 (2022).
[21] F. Forster, G. Petersen, S. Manus, P. Hänggi, D. Schuh, W. Wegscheider, S. Kohler, and S. Ludwig, Characterization of Qubit Dephasing by Landau-Zener-Stückelberg-Majorana Interferometry, Phys. Rev. Lett. **112**, 116803 (2014).
[22] M. D. Shulman, S. P. Harvey, J. M. Nichol, S. D. Bartlett, A. C. Doherty, V. Umansky, and A. Yacoby, Suppressing qubit dephasing using real-time Hamiltonian estimation, Nat. Commun. **5**, 5156 (2014).

[23] J. Preskill, Quantum computing in the NISQ era and beyond, Quantum **2**, 79 (2018).
[24] A. Blais, R.-S. Huang, A. Wallraff, S. M. Girvin, and R. J. Schoelkopf, Cavity quantum electrodynamics for superconducting electrical circuits: An architecture for quantum computation, Phys. Rev. A **69**, 062320 (2004).
[25] D. I. Schuster, A. Wallraff, A. Blais, L. Frunzio, R.-S. Huang, J. Majer, S. M. Girvin, and R. J. Schoelkopf, ac Stark Shift and Dephasing of a Superconducting Qubit Strongly Coupled to a Cavity Field, Phys. Rev. Lett. **94**, 123602 (2005).
[26] D. Schuster, A. A. Houck, J. A. Schreier, A. Wallraff, J. M. Gambetta, A. Blais, L. Frunzio, J. Majer, B. Johnson, M. H. Devoret, S. M. Girvin, and R. Schoelkopf, Resolving photon number states in a superconducting circuit, Nature (London) **445**, 515 (2007).
[27] X. Mi, M. Benito, S. Putz, D. M. Zajac, J. M. Taylor, G. Burkard, and J. R. Petta, A coherent spin–photon interface in silicon, Nature (London) **555**, 599 (2018).
[28] G. Burkard and J. R. Petta, Dispersive readout of valley splittings in cavity-coupled silicon quantum dots, Phys. Rev. B **94**, 195305 (2016).
[29] X. Mi, C. G. Péterfalvi, G. Burkard, and J. R. Petta, High-Resolution Valley Spectroscopy of Si Quantum Dots, Phys. Rev. Lett. **119**, 176803 (2017).
[30] A. Wallraff, D. Schuster, A. Blais, L. Frunzio, R.-S. Huang, J. Majer, S. Kumar, S. M. Girvin, and R. J. Schoelkopf, Strong coupling of a single photon to a superconducting qubit using circuit quantum electrodynamics, Nature (London) **431**, 162 (2004).
[31] J. J. Viennot, M. C. Dartiailh, A. Cottet, and T. Kontos, Coherent coupling of a single spin to microwave cavity photons, Science **349**, 408 (2015).
[32] A. Stockklauser, P. Scarlino, J. V. Koski, S. Gasparinetti, C. K. Andersen, C. Reichl, W. Wegscheider, T. Ihn, K. Ensslin, and A. Wallraff, Strong Coupling Cavity QED with Gate-Defined Double Quantum Dots Enabled by a High Impedance Resonator, Phys. Rev. X **7**, 011030 (2017).
[33] J. V. Koski, A. J. Landig, M. Russ, J. C. Abadillo-Uriel, P. Scarlino, B. Kratochwil, C. Reichl, W. Wegscheider, G. Burkard, M. Friesen, S. N. Coppersmith, A. Wallraff, K. Ensslin, and T. Ihn, Strong photon coupling to the quadrupole moment of an electron in a solid-state qubit, Nat. Phys. **16**, 642 (2020).
[34] C. L. Degen, F. Reinhard, and P. Cappellaro, Quantum sensing, Rev. Mod. Phys. **89**, 035002 (2017).
[35] J. Bylander, S. Gustavsson, F. Yan, F. Yoshihara, K. Harrabi, G. Fitch, D. G. Cory, Y. Nakamura, J.-S. Tsai, and W. D. Oliver, Noise spectroscopy through dynamical decoupling with a superconducting flux qubit, Nat. Phys. **7**, 565 (2011).
[36] J. Yoneda, K. Takeda, T. Otsuka, T. Nakajima, M. R. Delbecq, G. Allison, T. Honda, T. Kodera, S. Oda, Y. Hoshi, N. Usami, K. M. Itoh, and S. Tarucha, A quantum-dot spin qubit with coherence limited by charge noise and fidelity higher than 99.9%, Nat. Nanotechnol. **13**, 102 (2018).
[37] L. Petit, J. M. Boter, H. G. J. Eenink, G. Droulers, M. L. V. Tagliaferri, R. Li, D. P. Franke, K. J. Singh, J. S. Clarke, R. N. Schouten, V. V. Dobrovitski, L. M. K. Vandersypen, and M. Veldhorst, Spin Lifetime and Charge Noise in Hot Silicon Quantum Dot Qubits, Phys. Rev. Lett. **121**, 076801 (2018).
[38] R. Jock, N. Jacobson, M. Rudolph, D. R. Ward, M. S. Carroll, and D. R. Luhman, A silicon singlet–triplet qubit driven by spin-valley coupling, Nat. Commun. **13**, 641 (2022).
[39] E. Connors, J. Nelson, L. Edge, and J. Nichol, Charge-noise spectroscopy of Si/SiGe quantum dots via dynamically-decoupled exchange oscillations, Nat. Commun. **13**, 940 (2022).
[40] See Supplemental Material at http://link.aps.org/supplemental/10.1103/PhysRevLett.128.236801 for details on the quantum Langevin equations, the moments of the transmission, the extraction of the averaged noise integral, the transmission in the presence of a fluctuating qubit-photon coupling constant, the exemplary case of semiconductor charge qubits, and the extraction of the noise power spectral density from the averaged noise integral.
[41] As shown in Ref. [40], the qubit decoherence rate reads $\gamma = \coth(\omega_q/2T)\gamma_1 + 2\gamma_\varphi$ with zero-temperature relaxation rate γ_1 and dephasing rate γ_φ. When solving the full Lindblad equation to obtain the numerical data points in Fig. 2, we set $(\gamma_1, \gamma_\varphi) = [5\tanh(\omega_q/2T), 2.5]10^{-2}\delta_0$ in (a) and (b), $(\gamma_1, \gamma_\varphi) = [5\tanh(\omega_q/2T), 2.5]10^{-3}\delta_0$ in (c), and $(\gamma_1, \gamma_\varphi) = [0.5\tanh(\omega_q/2T), 0.25]\gamma$ in (d).
[42] M. J. Collett and C. W. Gardiner, Squeezing of intracavity and traveling-wave light fields produced in parametric amplification, Phys. Rev. A **30**, 1386 (1984).
[43] C. W. Gardiner and M. J. Collett, Input and output in damped quantum systems: Quantum stochastic differential equations and the master equation, Phys. Rev. A **31**, 3761 (1985).
[44] G. Burkard, M. J. Gullans, X. Mi, and J. Petta, Superconductor–semiconductor hybrid-circuit quantum electrodynamics, Nat. Rev. Phys. **2**, 129 (2020).
[45] J. Stehlik, Y.-Y. Liu, C. M. Quintana, C. Eichler, T. R. Hartke, and J. R. Petta, Fast Charge Sensing of a Cavity-Coupled Double Quantum Dot Using a Josephson Parametric Amplifier, Phys. Rev. Applied **4**, 014018 (2015).
[46] G. Zheng, N. Samkharadze, M. L. Noordam, N. Kalhor, D. Brousse, A. Sammak, G. Scappucci, and L. M. K. Vandersypen, Rapid gate-based spin read-out in silicon using an on-chip resonator, Nat. Nanotechnol. **14**, 742 (2019).
[47] E. J. Connors, J. J. Nelson, and J. M. Nichol, Rapid High-Fidelity Spin-State Readout in Si/Si-Ge Quantum Dots via rf Reflectometry, Phys. Rev. Applied **13**, 024019 (2020).
[48] F. Borjans, X. Mi, and J. R. Petta, Spin Digitizer for High-Fidelity Readout of a Cavity-Coupled Silicon Triple Quantum Dot, Phys. Rev. Applied **15**, 044052 (2021).
[49] L. Chirolli and G. Burkard, Decoherence in solid-state qubits, Adv. Phys. **57**, 225 (2008).
[50] J. Bergli, Y. M. Galperin, and B. L. Altshuler, Decoherence in qubits due to low-frequency noise, New J. Phys. **11**, 025002 (2009).
[51] Y. Makhlin and A. Shnirman, Dephasing of Solid-State Qubits at Optimal Points, Phys. Rev. Lett. **92**, 178301 (2004).

[52] V. Derakhshan Maman, M. F. Gonzalez-Zalba, and A. Pályi, Charge Noise and Overdrive Errors in Dispersive Readout of Charge, Spin, and Majorana Qubits, Phys. Rev. Applied **14**, 064024 (2020).

[53] L. Kranz, S. K. Gorman, B. Thorgrimsson, Y. He, D. Keith, J. G. Keizer, and M. Y. Simmons, Exploiting a single-crystal environment to minimize the charge noise on qubits in silicon, Adv. Mater. **32**, 2003361 (2020).

[54] K. D. Petersson, J. R. Petta, H. Lu, and A. C. Gossard, Quantum Coherence in a One-Electron Semiconductor Charge Qubit, Phys. Rev. Lett. **105**, 246804 (2010).

[55] P. Dutta and P. M. Horn, Low-frequency fluctuations in solids: $(1/f)$ noise, Rev. Mod. Phys. **53**, 497 (1981).

[56] E. J. Connors, J. J. Nelson, H. Qiao, L. F. Edge, and J. M. Nichol, Low-frequency charge noise in Si/SiGe quantum dots, Phys. Rev. B **100**, 165305 (2019).

[57] G. Ithier, E. Collin, P. Joyez, P. J. Meeson, D. Vion, D. Esteve, F. Chiarello, A. Shnirman, Y. Makhlin, J. Schriefl, and G. Schön, Decoherence in a superconducting quantum bit circuit, Phys. Rev. B **72**, 134519 (2005).

[58] M. Russ and G. Burkard, Asymmetric resonant exchange qubit under the influence of electrical noise, Phys. Rev. B **91**, 235411 (2015).

[59] Y. Nakamura, Y. A. Pashkin, T. Yamamoto, and J. S. Tsai, Charge Echo in a Cooper-Pair Box, Phys. Rev. Lett. **88**, 047901 (2002).